Proceedings of GT2006
ASME Turbo Expo 2006: Power for Land, Sea and Air
May 8-11, 2006, Barcelona, Spain

GT2006-90778

A DESIGN TO INCREASE THE STATIC STIFFNESS OF HOLE PATTERN STATOR GAS SEALS

Dara W. Childs, The Leland T. Jordan Professor of Mechanical Engineering
Turbomachinery Laboratory, Texas A&M University, College Station, TX, 77843 USA
Yoon-Shik Shin, Graduate Research Assistant
John Wade, Rotordynamics Engineer, Capstone Turbine

ABSTRACT

An analysis is presented which shows that a deep groove located at about 60% along the axial length from the inlet will approximately double the static stiffness of a hole-pattern-stator, annular gas seal. Test results for a seal using this geometry generally confirm the correctness of this prediction. The groove also produces an increase in leakage by about 4% and a modest decrease in effective damping.

INTRODUCTION

Injection compressors require comparatively long annular seals with high pressure drops that have a significant impact on rotordynamics. The balance-piston seal for straight-through compressors usually absorbs the full head rise of the machine. For back-to-back machines, the division-wall seal normally takes about one half of the machine's head rise but deals with higher density gas.

Annular seals using smooth rotors and honeycomb (HC) stators have been used since the 1960s in some petrochemical compressors. Conventional aluminum labyrinths were replaced because of the corrosion resistance of a stainless steel honeycomb material. HC surfaces are normally made from high-temperature stainless steels that have been developed as abradable surfaces for tooth-on-rotor labyrinths in aircraft gas turbines. This material is unforgiving in a rubbing condition. In addition, long lead times are frequently involved in securing a custom-manufactured honeycomb seal for a compressor. In response to these circumstances, Yu and Childs [1] tested three aluminum hole-pattern (HP) stator seals. The seal with a hole-area density of 60% performed as well as previously tested honeycomb-stator seals. Moore et al. [2] recently reported test results for a back-to-back centrifugal compressor that used a hole-pattern center bushing seal (with a swirl brake) to remarkably good effect --- the compressor's stability characteristics improved with increasing differential pressure. One manufacturer of injection compressors uses an electrical discharging manufacturing process to produce a honeycomb pattern in an aluminum stator. Most manufacturers have shifted to aluminum HP stators and away from traditional HC.

Predictions from Kleynhans and Childs [3] two-control-volume model showed that HP seals had strongly frequency dependent stiffness and damping coefficients, and tests results have confirmed these predictions for HP [4] and HC [5] seals. The direct stiffness of the seals increases with increasing frequency and can produce high synchronous stiffness values. However, their static (zero frequency) stiffness can be low or negative. Lomakin [6] explained that the static stiffness of an annular seal arises via the sharing of the seal ΔP through the inlet-loss drop and the friction-factor gradient along the seal's length due to wall friction. As a seal's length is increased, the predicted static stiffness first rises and then falls, eventually becoming negative. Stator roughness that increases the wall friction factor contribution aggravates the negative static-stiffness problem. To avoid or minimize negative stiffness, at least one pump manufacturer modifies long liquid seals by adding one or more deep grooves, replacing one long seal with several shorter seals.

With compressors, convergent tapered geometries of the clearance have been used to increase direct static stiffness. Fleming [7] first suggested this approach. However, a convergent taper also increases leakage and reduces the direct damping. In the present paper, analysis and tests are presented for an HP-stator seal with a single deep groove. Also, comparisons are made to predictions for the grooved seal and a convergent-tapered seal.

SEAL REACTION-FORCE / MOTION MODEL

For motion about a centered position, Kleynhans and Childs [3] developed the following reaction-force/relative-motion model for hole-pattern and honeycomb seals,

$$-\begin{Bmatrix} f_{sX}(s) \\ f_{sY}(s) \end{Bmatrix} = \begin{bmatrix} G & E \\ -E & G \end{bmatrix} \begin{Bmatrix} X(s) \\ Y(s) \end{Bmatrix} \qquad (1)$$

Here, *s* is the Laplace domain variable, $\boldsymbol{f_s}$ is the reaction force vector, and ***X(s)***, ***Y(s)*** are the Laplace-domain components of the relative displacement vector between the seal's rotor and stator. In terms of frequency-dependent stiffness and damping coefficients, the seal model looks like

$$-\begin{Bmatrix} f_{sX} \\ f_{sY} \end{Bmatrix} = \begin{bmatrix} K(\Omega) & k(\Omega) \\ -k(\Omega) & K(\Omega) \end{bmatrix} \begin{Bmatrix} X \\ Y \end{Bmatrix} + \begin{bmatrix} C(\Omega) & c(\Omega) \\ -c(\Omega) & C(\Omega) \end{bmatrix} \begin{Bmatrix} \dot{X} \\ \dot{Y} \end{Bmatrix} \qquad (2)$$

The two models are related by $\boldsymbol{G(j\Omega)} = K(\Omega) + \boldsymbol{j}C(\Omega)$, $\boldsymbol{E(j\Omega)} = k(\Omega) + \boldsymbol{j}c(\Omega)$, where $\boldsymbol{j} = \sqrt{-1}$. In comparing the rotordynamic performance of seals, the effective damping coefficient,

$$C_{eff}(\Omega) = C(\Omega) - k(\Omega)/\Omega, \qquad (3)$$

is very helpful, combining the stabilizing direct damping and destabilizing cross-coupled stiffness coefficients. This definition only applies for small motion about a centered position. The primary interest in this development is maximizing the static stiffness $K_{\boldsymbol{static}} = K(0)$.

OPTIMUM LOCATION FOR A SINGLE DEEP GROOVE

A code based on [3] was modified to account for a single groove at an arbitrary axial location within a seal. The groove was assumed to be large enough to isolate the two seal segments. Specifically, rotor motion was assumed to produce zero pressure oscillations in the groove. The analysis could handle exit recovery at the groove, but zero pressure recovery was assumed at the ends of both seal segments. The exit pressure from segment 1 was the supply pressure for segment 2, and flow continuity was preserved. The analysis was applied to the HP seal geometry of figure 1 with R =57.37 mm, and L = 86.06 mm, C_r = 0.20 mm, P_{in} = 70 bars, and $PR = P_{ex}/P_{in} = 0.5$. Figure 2 shows that placing the groove at approximately 60% of the seal length from the seal entrance produces the maximum $K_{\boldsymbol{static}}$.

The grooved test seal was made from an existing HP seal with the geometry of figure 1, except, the hole depth was H_d = 3.18 mm. The photograph in figure 3 illustrates the modification. The groove width and depth are both 5.5mm. CFD predictions showed that these dimensions realized a substantial pressure drop. Before the groove was added, this seal displayed strong negative static stiffness that forced a reduction in the supply pressure and limited the range of pressure drops that could be tolerated.

Seal divergence is known to cause negative stiffness. The dimensions of all seals tested in this program have been measured after being fitted into the test housing, and no measurable divergence has been detected. During tests, the axial pressure distribution tends to create larger clearances at the inlet leading to a converging flow path rather than a diverging flow path. Calculated increases in the clearances due to pressurization are smaller than the machining tolerances for manufacture. Also, the gas expansion normally creates a significant drop in temperature as the gas moves down the seal. Again, this temperature distribution would cause a convergent flow condition with tighter exit clearances.

The "friction-factor jump" phenomenon observed by Ha and Childs [8] and discussed by Ha et al. [9] provides one explanation for negative static stiffness. Specifically, these references cite flat-plate test results for which the friction factor increases with increasing Reynolds numbers at $R_e \geq 20000$; i.e., $\partial f_f / \partial R_e < 0$. The Lomakin effect [10] predicts a positive direct static stiffness for $\partial f_f / \partial R_e < 0$ and a reduced or negative stiffness for $\partial f_f / \partial R_e < 0$. For $\partial f_f / \partial R_e < 0$, the positive stiffness results from the sharing of the total seal ΔP between the inlet loss and the wall losses due to flow friction. For $\partial f_f / \partial R_e > 0$ moving the rotor away from a centered position causes a reduction of the reaction forces on the increased-clearance region and an increase in reaction forces on in the decreased-clearance areas.

TEST APARATUS AND PARAMETER IDENTIFICATION

The test apparatus has been described in several prior publications — Dawson et al. [11] and Weatherwax and Childs [12] including a discussion of relative uncertainty. The parameter identification approach is described by Rouvas and Childs [13].

TEST RESULTS

Childs and Wade's HP seal with H_d =3.30 mm was identical to the starting-point seal of figure 3 that had H_d = 3.18 mm but it displayed no negative stiffness problems and could be tested to the full available supply pressure. In the comparison seals that follow, results will be presented for this H_d = 3.30 mm seal (designated TEST), the modified grooved seal of figure 3 with H_d = 3.18 mm (designated TEST-G) and predictions. (Unfortunately, the H_d = 3.18 mm test data are proprietary and cannot be shown here.) The grooved seal had no negative-stiffness behavior. In all cases, the following conditions apply: zero preswirl, P_{in} = 70 bars, $PR \cong 0.5$. The code uses a Blasius friction-factor model of the form $f_f = nR^m$. The following coefficients are used for the rotor and stator, respectively m_r = -0.217, n_r = 0.0586, n_s = 0.035, m_s = -0.1101. These parameters are based on flat-plate results of Ha and Childs.

Figure 4 shows test results for $K_{eff}(f\Omega/\omega)$ for the grooved and ungrooved seal plus predictions for both seals. The grooved seal has higher projected static stiffness than the original seal, but significantly lower stiffness values for f >0.2. The code does a good job in predicting *K* for both the grooved and ungrooved seals.

Figure 5 provides predictions and measurement results for $C(f=\Omega/\omega)$, showing that the grooved seal has much lower *C* values at reduced frequencies, but approximately equal values at $f \cong .7$ and higher for higher values for *f*. Again, damping is well predicted for both seals. Figure 6 provides predictions and measurement results for $k(f=\Omega/\omega)$, showing that the grooved seal has lower *k* values at reduced frequencies, but approximately equal values at $f \cong .7$ and higher for higher values for *f*. The predictions are good for the original seal, but the measured *k* values for the grooved seal are significantly higher than predicted.

Figure 7 shows predictions and measurements for $C_{eff}(f)$. At low frequencies, C_{eff} is negative (due to *k*) but changes sign and becomes positive for higher frequencies. The grooved seal has a higher cross-over frequency and generally lower effective damping than the reference seal. For both seals, peak damping is over predicted, and the cross-over frequency is under predicted.

Figure 8 illustrates the seals' leakage coefficient,

$$\Phi = \frac{\dot{m}\sqrt{R_g T_{in}}}{\pi D C_r \Delta P};$$

versus ΔP where $\dot{m}$ is the mass flow rate, R_g is the gas constant, and T_{in} is the inlet temperature. The grooved seal leaks modestly more that the ungrooved seal. In compressor applications, the expected pressure ratios are on the order of 0.4~0.6. The supply pressure for figure 7 is 70 bars, so the lowest ΔP results are closest to compressor-application pressure ratios, and they correspond to an approximate 3% increase in leakage due to the groove. Both seals leak less than predicted.

DISCUSSION

The grooved-seal analysis works well in predicting an increase in static stiffness and the general rotordynamic characteristics of the grooved test seal. Aside from enhanced static stiffness, the grooved seal design does not compare favorably to the reference constant-clearance seal. Except at the lowest frequencies, it has lower direct stiffness values. At low frequencies it also has significantly lower direct damping. The effective damping is also lower for $f \leq 1$. The groove geometry tested here could be readily implemented into either conventional honeycomb seals or hole pattern seals that use honey-comb shaped cells.

As noted earlier, Fleming suggested a convergent taper to increase an annular seal's static stiffness. The following nondimensional parameter is useful in defining a seal's taper

$$q = \frac{C_{rin} - C_{rex}}{C_{rin} + C_{rex}}$$

We will examine the impact of converging taper on a compressor seal with the following characteristics: Discharge Pressure = 150 bar, Supply Pressure= 90 bar, Supply Temperature=100 C, ω = 10000 rpm, *D* = 150 mm, *L* = 150 mm, C_{rex} =x 0.2 mm, h_d = 3.3 mm, γ = 0.69, and an inlet preswirl ratio of zero, reflecting an effective swirl brake. The inlet radial clearance variation, $C_{rin} = 0.2, 0.3, 0.4, 0.5\ mm$, is used to produce q = 0, 0.2, .333, .429 .

Figure 9 illustrates K_{eff} versus Ω for this set of *q* values. Clearly, the predicted static stiffness values increase sharply with increasing *q*. At the highest taper value, K_{eff} is largely frequency independent. Tests by Dawson [14] confirm the behavior predicted in figure 9 for q = 0.429.

Figure 10 illustrates the ratio of predicted static stiffness and leakage between convergent-tapered seals and a constant clearance seal. Figure 2 showed that an optimally-spaced groove can double the static stiffness of a long constant-clearance seal. From figure 10, a taper parameter of q = 0.04 will also double the static stiffness. This taper will increase the leakage by about 3%. Hence, for the seal considered, the grooved seal and an equivalent tapered seal will produce about the same increase in K_{static} and $\dot{m}$.

Figure 11 illustrates predicted values for C_{eff} for a range of *q* values showing the drop in damping with increasing taper. Note that increasing the taper parameter also increases the cross-over frequency.

CONCLUSIONS

Test results presented here confirm that a deep axial groove at about 60% of the axial length from a seal inlet will produce a significant increase in static stiffness. The grooved seal leaks approximately 3% more than an unmodified seal and has a reduced effective damping coefficient. Similar performances are predicted for convergent tapered geometries with a small taper parameter, and significantly higher static stiffness values are theoretically achievable for tapered-bore seals.

NOMENCLATURE

C_r	Radial clearance	[L]
C, c	Direct and cross-coupled damping coefficient	[FT/L]
C_{eff}	Effective damping coefficient, Eq.(3)	[FT/L]
$\mathbf{f_s}$	Seal reaction force	[F]
H_d	Hole depth	[L]
$\boldsymbol{H_{ij}}$	Dynamic stiffness coefficient	
K, k	Direct and cross-coupled stiffness fficients	[F/L
Ω	Rotor precession frequency at seal location	[1/T]
ω	Running speed	[1/T]

REFERENCES

[1] Yu, Z., and Childs, D. W. , "A Comparison of Experimental Rotordynamic Coefficients and Leakage Characteristics Between Hole-Pattern Gas Damper Seals and a Honeycomb Seal," *ASME J. of Engineering for Gas Turbines and Power*, **120**, No. 4, pp. 778-783, October 1998.

[2] Moore, J., Walker, S., and Kuzdal, M., "Rotordynamic Stability Measurements During Full Load Testing of a 6000 psi Reinjection Centrifugal Compressor," Proceedings, 31st Texas A&M University Turbomachinery Symposium, pp 29-38, September 2002.

[3] Kleynhans, G., and Childs, D., "The Acoustic Influence of Cell Depth on the Rotordynamic Characteristics of Smooth-Rotor/Honeycomb-Stator Annular Gas Seals," *ASME Journal of Engineering for Gas Turbines and Power*, **119**, No. 4, pp. 949-957, October 1997

[4] Childs, D. and Wade, J., "Rotordynamic-Coefficient and Leakage Characteristics for Hole-Pattern-Stator Annular Gas Seals — Measurements versus Predictions,"*ASME J. of Tribology*, pp. 326-333, **126**, No. 2, April 2004.

[6] Sprowl, B. and Childs, D., "A Study of the Effects of Inlet Preswirl on the Dynamic Coefficients of a Straight-Bore Honeycomb Gas Damper Seal," paper GT2004-53328 ASME IGTI Conference, Vienna, Austria, June 2004

[6] Lomakin , A., "Calculation of Critical Numbers of Revolutions and the Conditions Necessary for Dynamic Stability of Rotors in High-Pressure Hydraulic Machines when Taking into Account Forces Originating in Sealings," *Power and Mechanical Engineering*, April 1958 (in Russian)

[7] Fleming, D., 1979, "Stiffness of Straight and Tapered Annular Gas Seals," ASME *Journal of Lubrication Technology*, **101**, No.3, pp. 349-355.

[8] Ha, T. W., Childs, D. W., "Friction-Factor Data for Flat-Plate Tests of Smooth and Honeycomb Surfaces," *ASME J. of Tribology*, **14**, pp. 722-730, October 1992.

[9] Ha, T.-W., Morrison, G., Childs, D., "Friction-Factor Characteristics for Narrow-Channels with Honeycomb Surfaces," *ASME J. of Tribology*, **114**, pp. 722-730, October 1992.

[10] Lomakin , A., "Calculation of Critical Numbers of Revolutions and the Conditions Necessary for Dynamic Stability of Rotors in High-Pressure Hydraulic Machines when Taking into Account Forces Originating in Sealings," *Power and Mechanical Engineering*, April 1958 (in Russian)

[11] Dawson, M., Childs, D., Holt, C., and Phillips, S.,"Theory versus Experiments for the Dynamic Impedances of Annular Gas Seals: Part 1-Test Facility and Apparatus,"*ASME J. of Gas Turbines and Power*, **24**, pp. 958-963, October 2002

[12] Weatherwax, M., and Childs, D., "The Influence of Eccentricity on the Leakage and Rotordynamic Coefficients of a High Pressure, Honeycomb, Annular Gas Seal ... Measurements Versus Predictions," *ASME J. of Tribology*, **125**, pp. 422-429, April 2003.

[13] Rouvas, C. and Childs, D., "A Parameter Identification Method for the Rotordynamic Coefficients of a High Reynolds Number Hydrostatic Bearing," *ASME J. of Vibration and Acoustics*, **115**, pp. 264-270, July 1993.

[14] Dawson, M., A Comparison of the Static and Dynamic Characteristics of Straight Bore and Convergent Tapered-Bore Honeycomb Annular Seals, M.S. Thesis, Texas A&M University, May 2000.

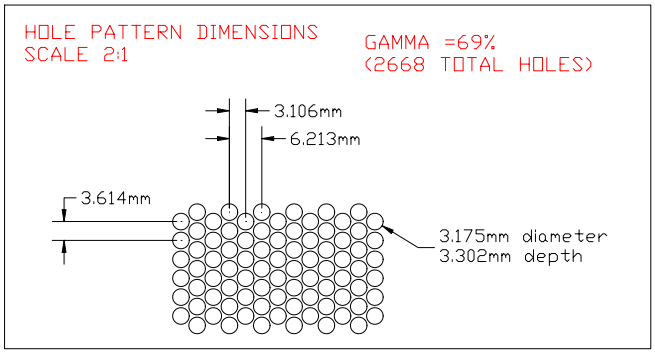

Figure 1 Hole-pattern geometry

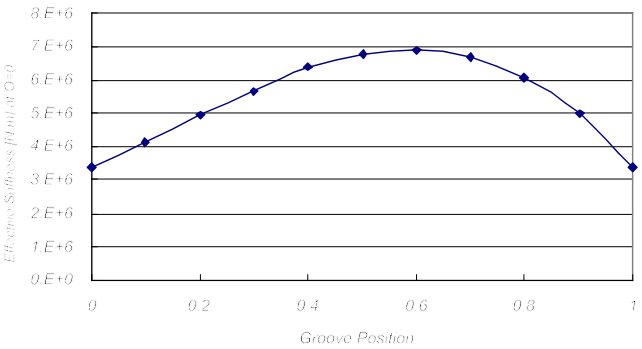

Figure 2 K_{static} versus axial groove location.

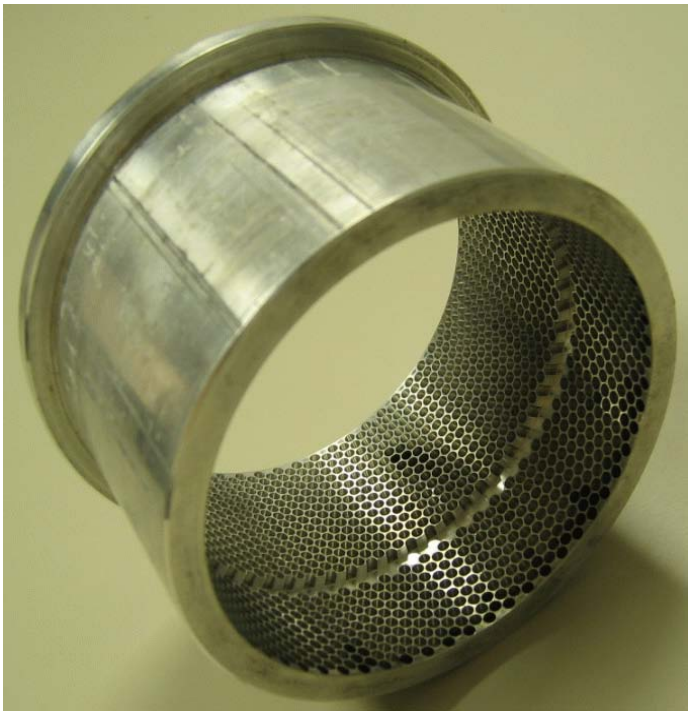

Figure 3 Seal with groove

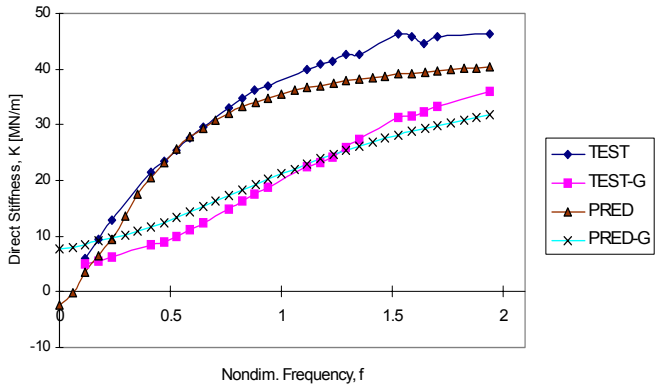

Figure 4 K_{eff} test results and predictions for the reference ungrooved seal and the grooved seal of figure 3.

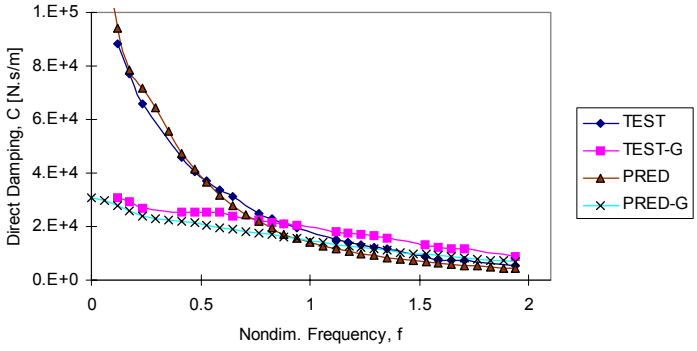

Figure 5 *C* test results and predictions for the reference ungrooved seal and the grooved seal of figure 3

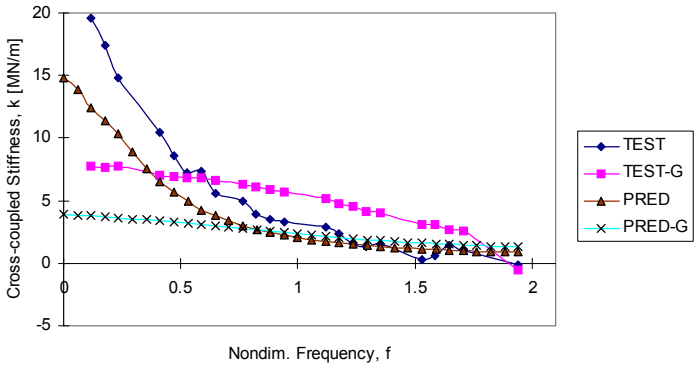

Figure 6 *k* test results and predictions for the reference ungrooved seal and the grooved seal of figure 3.

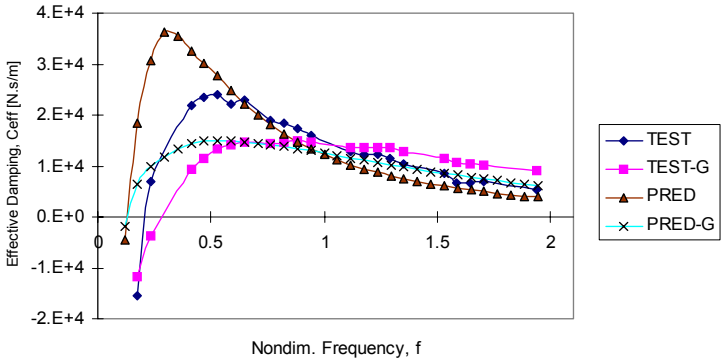

Figure 7 C_{eff} test results and predictions for the reference ungrooved seal and the grooved seal of figure 3

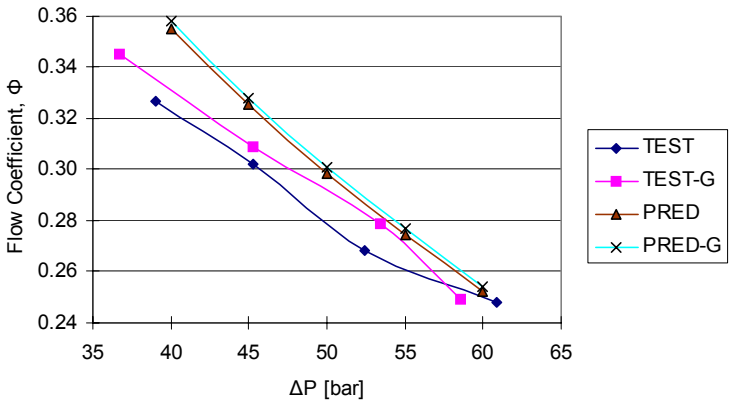

Figure 8 **M** predictions and measurements versus **)**P for the reference ungrooved seal and the figure 3 grooved seal

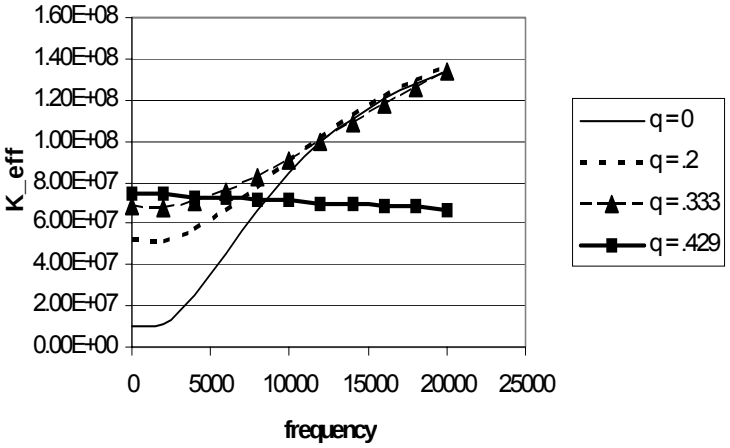

Figure 9 K_{eff} versus **S** for a range of *q* values

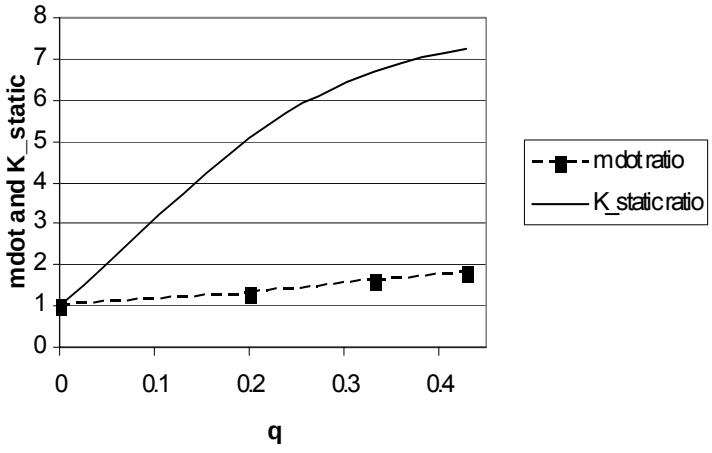

Figure 10 Predicted ratio between constant clearance and convergent taper geometries for K_{static} and $\dot{m}$

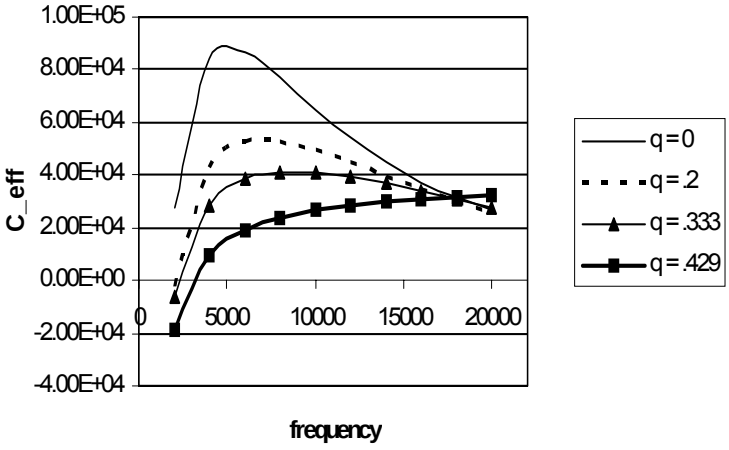

Figure 11 C_{eff} versus **S** for a range of *q* values

6